ELSEVIER

Physica A 220 (1995) 357–375

PHYSICA A

Two dimensional chemical pattern formation in gels. Experiments and computer simulation

A. Büki*, É. Kárpáti-Smidróczki, M. Zrínyi

Technical University of Budapest, Department of Physical Chemistry, H-1521, Budapest, Hungary

Received: 2 May 1995

Abstract

Precipitate forming chemical reactions have been studied in chemically cross-linked poly(vinyl-alcohol) gel layers and in thin silica films. One of the reactive components was incorporated into the gel, the other was allowed to diffuse into the film. This reaction–diffusion process resulted in patterns that were different in some respects from that of the regular Liesegang phenomena often occurring in such systems. Instead of stripes, tree-like precipitate structures have developed. Digital image analysis provided evidence that the tree-like structures involve a periodicity of the Liesegang type. Occurrence of this periodicity was found not only parallel but also perpendicular to the direction of the diffusion. Computer simulations were carried out in order to find possible mechanisms for these variants of the Liesegang phenomenon and to establish the influence of various factors on the chemical pattern formation involved in the model.

1. Introduction

It has long been known that those reactive systems in which the reactants are transported by diffusion often result in pattern formation. As a result of the reaction–diffusion process, chemical patterns can occur intermittently in terms of time and space or both [1].

The Liesegang phenomenon [2] is one of the most frequently studied examples of rhythmic precipitate formation occurring in gels. In a usual Liesegang experiment two electrolytes react with each other in a gel providing a nonsoluble material. The process is not instantaneous, because a part of the reacting materials is incorporated into the gel media whereas the other is allowed to diffuse into it. Normally, the gel is prepared in a test tube mixed with one of the reactive electrolytes, and the other solution is poured on top of the gel cylinder. The main role of the gel is to prevent

* Corresponding author

SSDI 0378-4371(95)00146-8

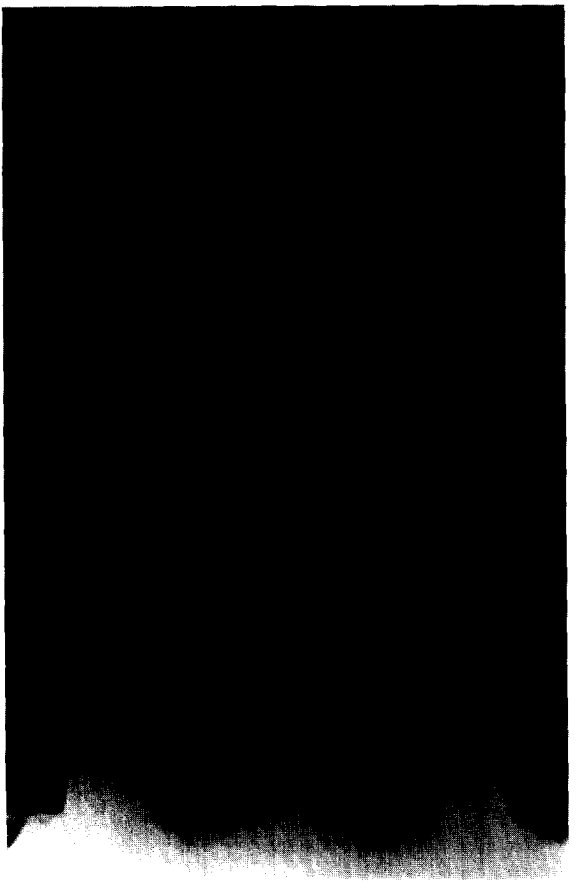

Fig. 1. A regular Liesegang pattern of $Mg(OH)_2$ formed in PVA gel.

sedimentation of the precipitate as well as the convection of the reactants. Thus, the mechanism of the transport process becomes effective and the chemical reaction is coupled with diffusion.

One would expect that the insoluble product (precipitate) forms an ever-broadening, continuous region as the diffusion proceeds. Under certain conditions, however, the reaction–diffusion process results in a special pattern, which consists of many well-distinguishable precipitate zones (stripes) as shown in Fig. 1. This pattern formation was discovered more than a century ago, and was studied experimentally and theoretically by many authors [2–8].

Fig. 1 shows some periodic spatial structures formed of $Mg(OH)_2$ in PVA gel. Instead of a continuous precipitate zone, a series of precipitate bands occur perpendicularly to the direction of the diffusion. In most cases, the distances of the bands (X_i) (measured from the gel surface or from each other) can be considered as members of

a geometrical series with a quotient P, named the spacing coefficient of the structure [3]:

$$P = X_{i+1}/X_i. \tag{1}$$

The above equation is often regarded as Jablczinsky's spacing law. The pattern formation shows a certain regularity in time as well [3]:

$$P_t = X_i/\bar{t}_i = \text{constant}, \tag{2}$$

where t_i denotes the time elapsed until formation of the ith band.

Many experiments have been carried out in test tubes in order to understand the influence of internal and external electrolyte concentrations on the spacing coefficient [9].

Only a few studies can be found in which Liesegang experiments are reported to be realized in thin films [10–12]. The great advantage of these experiments is that one can study the internal structure of the patterns with the aid of a light microscope or by other means.

The main purpose of the present work is to study several reaction–diffusion processes occurring in thin layers. We have performed many real experiments and two-dimensional simulations on the basis of chemical arguments. The results of the experiments and simulations were compared in order to get a deeper insight into the detailed mechanism of the chemical pattern formation.

2. Experimental part

Two types of gel media were applied in our experiments and two precipitate forming chemical reactions were studied in detail.

Poly(vinyl-alcohol) gels with a thickness of 0.2–1 mm were prepared by the cross-linking of primary poly(vinyl-alcohol) (PVA) chains with glutaric aldehyde (GDA) in an aqueous solution. Commercial PVA (Merck 821038) and solution of 25 wt% GDA (Merck) were used for the preparation. The initial polymer concentration as well as the cross-linking density were varied in order to obtain a highly swollen gel with suitable mechanical stability.

The precipitate-forming chemical reaction was realized by mixing one of the reactants with the polymer solution containing the cross-linking agent. The gelation process was induced through decreasing the pH of the system by adding some droplets of nitric acid (Carlo Erba). The solution was then poured onto glass plates. After completion of network formation the gel film, together with the holding glass plate was immersed into the solution of the other electrolyte to allow it to diffuse into the gel media. In each case the diffusion took place vertically and upwards. In fact, we tried out some other possible experimental setups, but no gravitational effects were observed.

In the other series of experiments commercial chromatographic silica thin layers (Merck Art. 5735 60 F254) were used as reaction media. In these cases the thin layer was at first totally immersed into the solution of the inner electrolyte for 30 minutes. Then the reaction took place in the same way as described above.
The chemical reactions we studied were the following:

$$Pb(NO_3)_2 + 2\,NaCl = PbCl_2 + 2\,NaNO_3$$

in chemically cross-linked PVA films, and:

$$Hg(NO_3)_2 + 2\,KI = HgI_2 + 2\,KNO_3$$

in silica thin layers.

$PbCl_2$ is a white precipitate which can slowly dissolve in the surplus of the NaCl solution. In the experiments $Pb(NO_3)_2$ was in the gel and NaCl played the role of the outer electrolyte, that is, it was allowed to diffuse into the gel.

HgI_2 is a yellow or deep-orange precipitate, depending on the stoichiometry. It can also redissolve in the surplus of the KI by complex formation.

3. Experimental results

All the experiments were carried out at room temperature. In the case of $PbCl_2$ a highly ramified tree-like precipitate structure was formed.

$PbCl_2$ forms small, needle-shaped crystals. The final structure in its entirety consists of these needles sized at about 1–2 mm. The crystals are arranged along continuous lines which start to grow at the bottom of the gel film where it is in contact with the other solution (NaCl) and propagate upwards by forming many ramifications. This pattern can be seen in Fig. 2.

At certain sites the growth process ceases abruptly. All of the branches stop growing at the same time and at the same distance from the beginning of the structure. They rest for a while and some of them abruptly start to grow again. These "survivors" propagate quickly and form many new branches. The other ones remain at the same place where they have stopped permanently. If we produce the horizontal density profile of such a structure by digital image analysis we get a function with many peaks at the places of stops, as can be seen in Fig. 3. The arrangement of the peaks fulfil the Jablczinsky relation, Eq. (1), Fig. 4, according to which it can be established that this structure is a special case of the Liesegang pattern formation. According to the image analysis this periodicity occurs also parallel to the direction of diffusion, that is, the area of the holes between the layers follows the same spacing law as the peaks in the density profile, as shown in Fig. 5.

When the Liesegang experiments produced HgI_2 in thin silica gel layers, an irregular structure was developed in all of the cases. These patterns consist of precipitate zones just like the usual Liesegang structures. However, one cannot find

Fig. 2. A highly ramified tree-like precipitate pattern of $PbCl_2$ formed in chemically crosslinked PVA gel film.

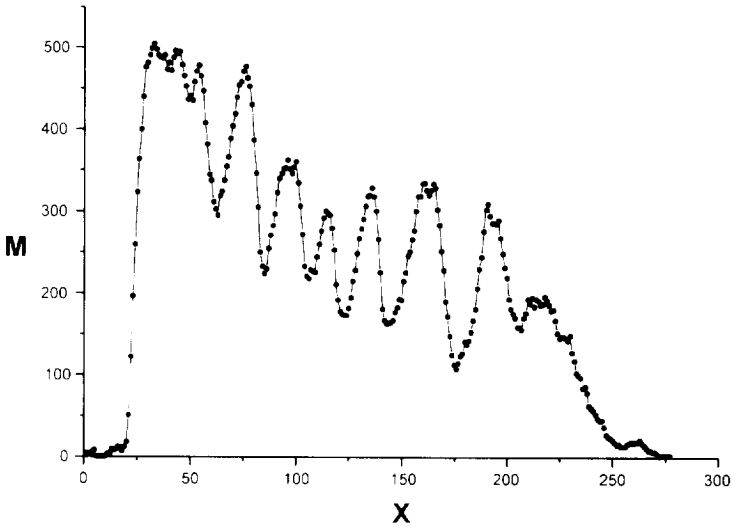

Fig. 3. The density profile of a tree-like precipitate pattern shown in Fig. 2, obtained by digital image processing.

any regularity in their arrangement. A typical instance of such structures and its density profile determined from a digitalized image of the plate are shown in Fig. 6.

If one examines these patterns with the naked eye all of them consist of randomly arranged, broad, diffuse bands. However, the spaces between the visible bands are

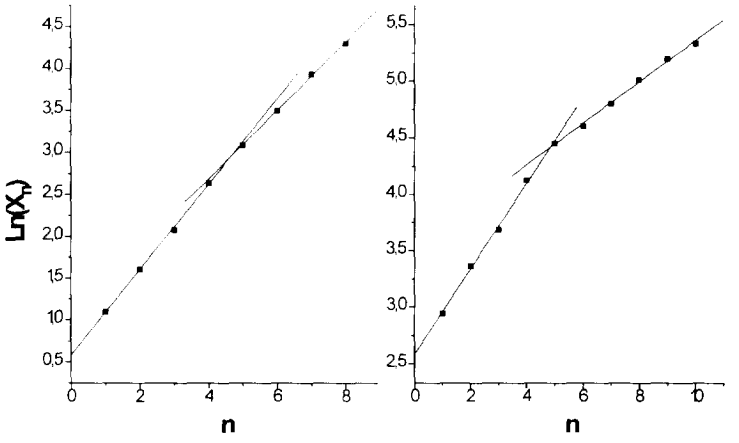

Fig. 4. The $\mathrm{Ln}(X_n)$ versus n function for a real (left curve) and a simulated (right curve) tree-like precipitate pattern. (The corresponding simulated structure can be seen in Fig. 11. The real structure is shown in Fig. 2).

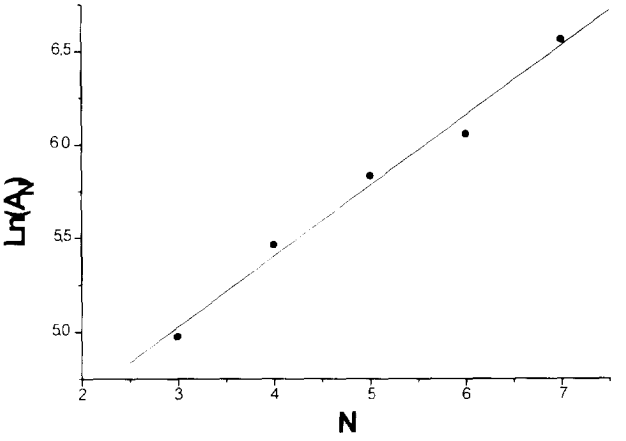

Fig. 5. The average area of the holes in a tree-like precipitate structure versus the number of the corresponding layers. The size distribution fulfils the Jablczinsky relation.

filled with a lower concentration of precipitate, which can be observed only with a light microscope with a magnification of 20. Such a microstructure is shown in Fig. 7.

The precipitated material in these diffuse areas is not evenly distributed but forms patches the size of which increases in the direction of the diffusion. These findings allow us to conclude that, contrary to Ostwald's supersaturation mechanism [13], in this system nucleation takes place continuously in space as was found in other systems by Kai et al. [14].

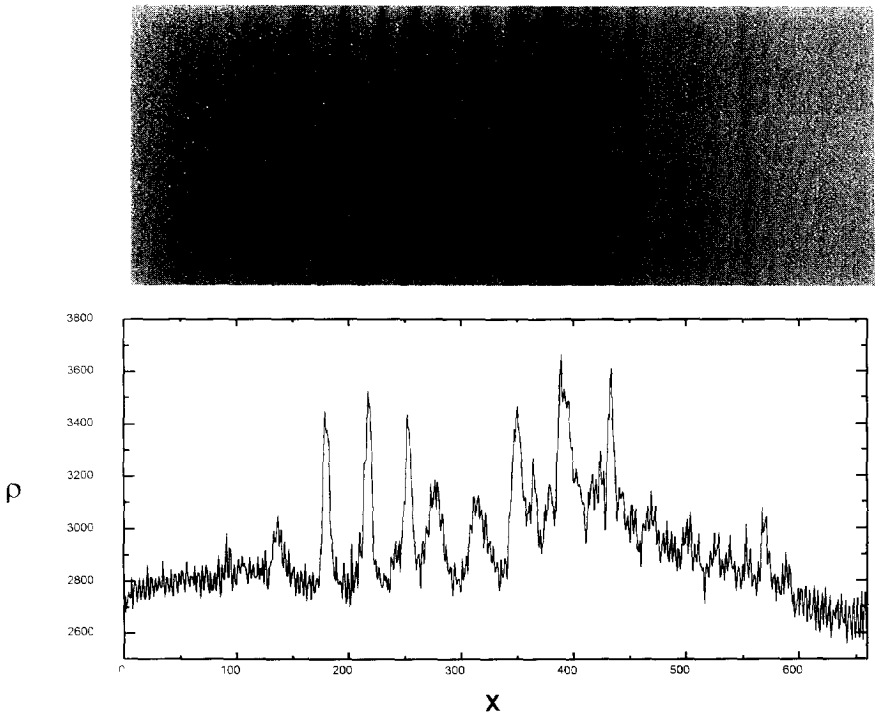

Fig. 6. An irregular pattern was formed of HgI_2 in a thin silica gel layer, and its density profile. The structure consists of randomly distributed strips and diffuse areas between them.

4. Simulation of the supersaturation model

The earliest explanation of the Liesegang phenomenon is referred to as the Ostwald supersaturation theory [3]. This is a rather simple mechanism in which it is supposed that the formation of the precipitate has two barriers. It is commonly known from analytical chemistry that a precipitate cannot come into existence until the concentration product of its solved ions reaches a certain level, the so-called "solubility product". The existence of such a thermodynamic barrier follows from the law of mass action.

However, it is also known that, in most cases, the formation of solid product does not start at this concentration level, because the formation of crystallites (nucleation) is a kinetically hindered process. This means that a (sometimes highly) supersaturated state preceeds the reaction. The kinetic barrier vanishes when the system contains some crystals of the precipitate, or some impurities which can catalyze the nucleation. At first, we tried to check the validity of this theory by 1D simulations.

When the Liesegang phenomenon is studied by computer simulation the main task is to solve a set of coupled reaction diffusion equations. Let us consider the simplest

Fig. 7. The microstructure of a diffuse region in a HgI_2 structure. The precipitate is not evenly distributed but forms patches the size of which increases in the direction of diffusion.

precipitate forming reaction:

$$A + B = AB.$$

In such a process the AB precipitate contains equal amounts of the components characterized by their concentrations C_A and C_B and thus

$$r = -dC_A/dt = -dC_B/dt = kC_AC_B, \tag{3}$$

where r denotes the velocity of the chemical reaction and k stands for the reaction rate constant. The coupled reaction–diffusion equations to be solved are:

$$\partial C_A/\partial t = D_A \partial^2 C_A/\partial x^2 - kC_AC_B, \tag{4a}$$

$$\partial C_B/\partial t = D_B \partial^2 C_B/\partial x^2 - kC_AC_B. \tag{4b}$$

In the above equations it is supposed that the diffusion can be described by Fick's second law. This second-order differential equation is often solved by the method of

finite differences which was applied earlier by other workers [7, 15]. The basis of this procedure is that the time and space intervals are divided into small steps (ΔX and Δt) of equal length and the first and second derivatives are approximated by their differences.

In the simulations the length and time were measured in arbitrary units. For the sake of simplicity ΔX and Δt were chosen equal to unity. This means that in our equations the nominal value of the diffusion constant can be calculated by the equation

$$D = D^*(\Delta X^*)^2/\Delta t^*, \tag{5}$$

where quantities marked with an asterisk are measured in real units. It can be easily shown that the numerical solution we get on this basis will be stable when the diffusion coefficient D falls between zero and 0.5 [7]. The accuracy of the solution can be verified by a well known rescaling property of the concentration profiles described in [16].

The Liesegang experiments are usually carried out in closed test tubes. This condition was fulfilled in the simulations by keeping the first derivative of the concentration profiles at zero at the boundary.

We can introduce similar simplifications in the description of the chemical reaction as well. If the reaction is much faster than the transport of the components the above set of kinetic equations can be generalized, taking into account the reaction terms as precipitate sinks with a threshold determined by the solubility product:

$$\partial C_A/\partial t = D_A \partial^2 C_A/\partial x^2 + \delta_A(L - C_A C_B), \tag{6a}$$

$$\partial C_B/\partial t = D_B \partial^2 C_B/\partial x^2 + \delta_B(L - C_A C_B), \tag{6b}$$

where L represents the precipitation product, which is a thermodynamic parameter characterizing a chemical reaction. When the product of the concentration of the two reactants exceeds this threshold, precipitate will form, until the concentrations decrease to the level determined by the solubility. However, this process can take place only if the crystal formation does not have a kinetic barrier. Practically, the latter means that the matrix has to contain some crystals which were formed earlier, or other inpurities which can catalyze the nucleation (see later). The function δ is defined by the equations

$$\delta_A(L - C_A C_B) = \begin{cases} 0 & \text{if } C_A C_B < L, \\ \delta C & \text{if } C_A C_B \geq L, \end{cases} \tag{7a}$$

$$\delta_B(L - C_A C_B) = \begin{cases} 0 & \text{if } C_A C_B < L, \\ \delta C & \text{if } C_A C_B \geq L, \end{cases} \tag{7b}$$

$$\delta C = \tfrac{1}{2}[(C_A + C_B) \pm \sqrt{(C_A + C_B)^2 - 4(C_A C_B - L)}]. \tag{7c}$$

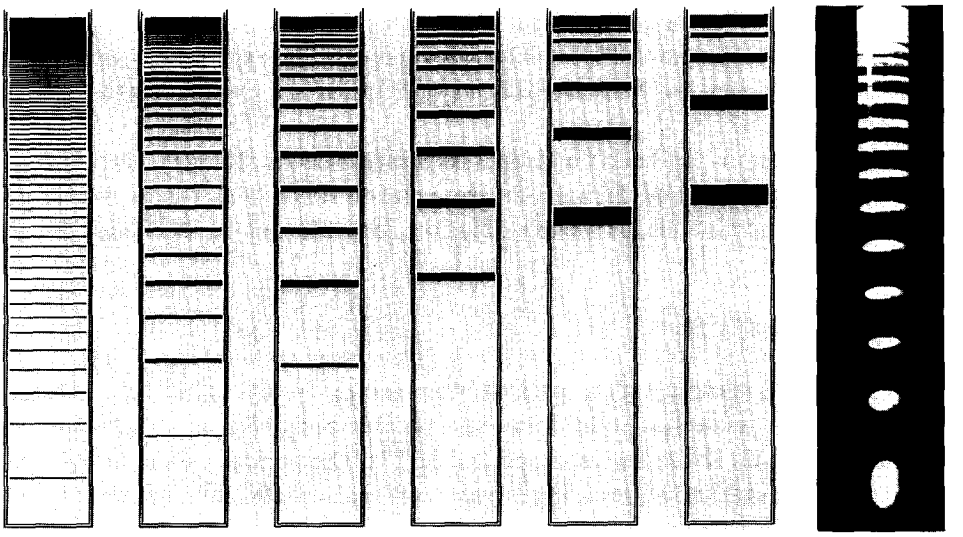

Fig. 8. Simulated Liesegang patterns with different nucleation products and a real structure. From left to right $K_s = 0.101, 0.103, 0.105, 0.110, 0.115, 0.130$).

Some one-dimensional, regular Liesegang structures simulated by this method together with a real structure can be seen in Fig. 8. The results obtained on the basis of the above-described mechanism are described in detail in our previous paper [17].

5. Simulation of irregular HgI_2 structures by means of a variant of the supersaturation model

According to our assumption, experimentally observed, spatially continuous precipitation occurs because nucleation is not purely governed by the supersaturation, as was supposed in the one-dimensional simulations [17]. The formation of a new crystallite can take place in two different ways. Nucleation can be induced by random concentration fluctuations or by the surface of a solid particle. The former case, which is governed purely by the degree of the supersaturation, is called "homogeneous" nucleation. The latter is referred to as "heterogeneous" nucleation. In the latter case the inducing surface can be a solid impurity, another precipitate crystal or the surface or the gel matrix.

In the numerical description of this irregular structure formation it was supposed that the nucleation in the system can take place in a homogeneous as well as a heterogeneous way. The former causes formation of the broad, dense stripes while the latter the diffuse regions between them.

It was not possible to reproduce the whole mechanism by simulation because of the lack of the theoretical background of homogeneous nucleation which occurs in this system. The possibility of redissolution of the precipitate by complex formation and

the unstoichiometric composition of the material makes the processes even more complicated. It has been supposed that the swelling of the silica particles, the different diffusion velocity of the electrolytes in the network and between the silica grains, and the specific adsorption or absorption of some ions play important roles as well. However we were able to reproduce the precipitate distribution of the diffuse regions based on a probabilistic variant of the supersaturation model.

We have applied mainly the same algorithm as described above. In one-dimensional simulation the velocity of the nucleation process was described by a simple step function.

In 2D the differential equation of diffusion was solved numerically on a triangular lattice, and unlike the 1D simulation, the nucleation was treated as a probabilistic process. In the description of the precipitation it was supposed that in the nucleation the inducing agent is the surface of the solid gel matrix, so the probability of its occurrence is a small constant value for the whole medium.

At every point where the product of the concentrations reached the nucleation product, but no precipitate had yet occurred the program performed a Monte-Carlo decision with respect to nucleation.

Fig. 9 shows some simulated precipitate distributions obtained by this mechanism. One can see that the size of the individual precipitates increases as the distance

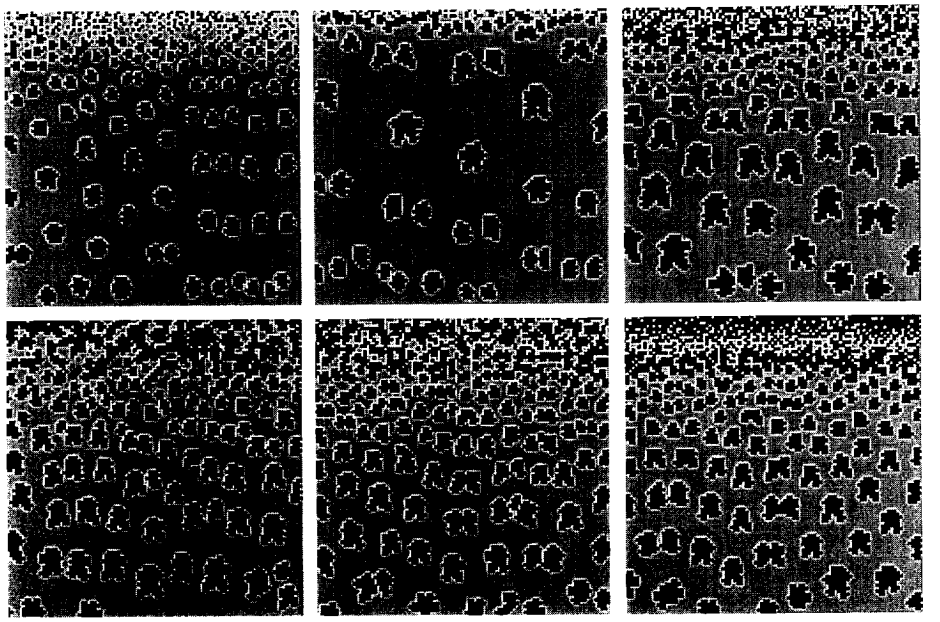

Fig. 9. Some simulated two-dimensional precipitate distributions were developed by the probabilistic variant of the supersaturation model. In some cases, a satellite strip can be seen in the pattern (lower right) which is characteristic of the real structures as well.

measured from the precipitate band increases, just as in the real structures (see Fig. 7). In some cases a satellite strip comes into existence after the dense precipitate region, which is characteristic of real structures as well.

6. Simulation of the highly ramified tree-like $PbCl_2$ structures

It has been supposed that a different mechanism is responsible for this special case of Liesegang pattern formation. On the basis of our experimental findings the following assumptions were taken into account in developing the appropriate simulation algorithm:

(1) The formation of tree-like line structures can be explained by the anisometric shape of the crystals. Because of their needle shape there is a favoured direction in the growth process which leads to the formation of lines and trees.

(2) The lines are continuous, which means that formation of new crystals can take place only on the surface of other ones. From this experimental finding we can conclude that, in this system, the nucleation has an exclusively heterogeneous mechanism.

(3) We have never seen a branch come into existence in an area where other branches exist. This means that the lines can grow only along their endpoints.

(4) The branches grow continuously upwards, which means that they cannot be governed by supersaturation because the points where the value of this parameter is the highest are arranged horizontally, not vertically. However, the branches "know" somehow, which direction is "upwards". This can be explained by the adsorption of the electrolytes on the crystal surfaces and their effect on surface energy [18]. Our hypothesis is that the inner and the outer electrolytes have an opposite effect on this energy so they change the probability of nucleation in opposite directions. The inner electrolyte promotes nucleation while the outer one hinders it. The latter assumption can be explained on the basis of our experimental findings because we have found that the surplus of the outer electrolyte dissolves the crystals. In the simulations it has been supposed that the parameter which governs the growth of branches is not the product of the concentrations but the average direction of their gradients.

(5) The growth mechanism sketched above cannot explain the abrupt stops in the process. There must be a kinetic effect in the system which can prevent the growth of the needles and the propagation of the branches.

It was found by Abdulkadhar et al. [19] that the growth of $PbCl_2$ single crystals can be divided into two phases. The former is a fast growth process but in the latter the process slows down significantly.

This finding can be proved if we suppose that the quality of the surface suffers a change during the growth process. At first, the crystal surface is rough and this is very favourable for heterogeneous nucleation. However, such a rough surface is not in equilibrium with its surroundings so it will smoothen during the growth process. After reaching a certain size the surface is too smooth to make nucleation possible. So after

this critical size crystal growth gradually diminishes, and finally, the propagation of the branches abruptly stops.

In our system such a state can come into existence many times because the propagation of the branches is faster than the diffusion of the outer electrolyte. So, the branches hurry forward where the supersaturation, and so the probability of nucleation, is smaller. This means that the propagation of branches stops but the growth of the crystals at the ends of some of the crystals will continue for a while. These crystals will reach the critical size mentioned above and the branches will rest at the same position. Growth is kinetically hindered in the whole system.

Only one question remains open: if the branches stop growing, why do they start to grow again? After the kinetically hindered state sets in, the diffusion of the electrolytes continues. So, a highly supersaturated region will form over the branches which cannot grow. On the other hand, the concentration of the outer electrolyte at the ends of branches will reach a value which is high enough to start the dissolution of these crystals. This effect makes the crystal surfaces rough again and, because the supersaturation of their surroundings is very high, a fast growth process starts. However, it is not valid for every part of the structure.

The branches which started earlier deplete the supersaturated region, so the others do not have enough material to survive. Although they are no longer in a kinetically hindered state they are not able to grow and will stop there forever.

On the basis of the above described mechanism we have developed a simulation algorithm. We have taken into account that the size of the crystals is commensurate with the thickness of the gel film, which means that the structure is continuously hindering the diffusion of the electrolytes. From a mathematical point of view this is a very difficult problem because the structure is continuously modifying the conditions of its own growth. However, in a numerical simulation it requires only a two-dimensional inhomogeneous diffusion algorithm which is easy to implement.

We have solved the differential equation of the diffusion on a triangular lattice in which each point had its own diffusion coefficient. This latter depended linearly on the amount of precipitate

$$D(X, Y, t) = D_{\max} - (D_{\max} - D_{\min}) M(X, Y, t) / M_{\max}, \tag{8}$$

where $D_{\max}$ and $D_{\min}$ are the minimal and maximal value of the diffusion coefficients (input parameters), M is the actual amount of the precipitate at the given site and time, and $M_{\max}$ is the maximal amount of precipitate which can form at a given point.

The spatial distribution of the diffusion coefficients was determined at every step of the iteration. In other respects the applied algorithm was a supersaturation model except that the formation of new crystal was subjected to two conditions: (1) a certain level of supersaturation and (2) the existence of a neighbouring lattice point where the amount of the precipitate was not zero (heterogeneous nucleation). The formation of the precipitate was probabilistic, that is, even if the above mentioned two conditions were fulfilled, precipitation could take place only if a random number generated by

the program was smaller than the probability of the nucleation. This latter was an input parameter.

Because of the anisometric character of the crystals, the algorithm stored for every lattice point the direction of the branch and the code of the kinetic state of the crystals (ready to grow or not) as additional information. Therefore a flag byte was used for this purpose (see Fig. 10).

The lowest bit was the sign of growth ability. If this bit was 1, the crystal at the given lattice point was growing, depending on the concentrations of the reactants. If the size of the crystal (that is the amount of the precipitate at that point) had reached a certain threshold (kinetically hindered state), or after reaching a certain size – a new nucleus was formed at one of the neighbouring points, this bit was set to 0. In the former case the crystal had the possibility to start again, if the concentration of the outer electrolyte reached the value which is required to slowly dissolve the crystal surface and so make it rough. If the concentration was high enough, the lowest bit was set back to 1. However this process was probabilistic, and the probability of such a "rebirth" was very low (0.01–0.05). This means that only a few crystals had a chance to start again from the hindered state, because the ones which were reborn earlier had depleted their surroundings.

The crystals in a kinetically hindered state always favored an upwards direction, and this information was stored on flag bits number 5 and 6. This slight restriction was required only to avoid traps of the other branches at the restart, and was applied only at the first step after the "rebirth", so hopefully did not really affect the entire growth process.

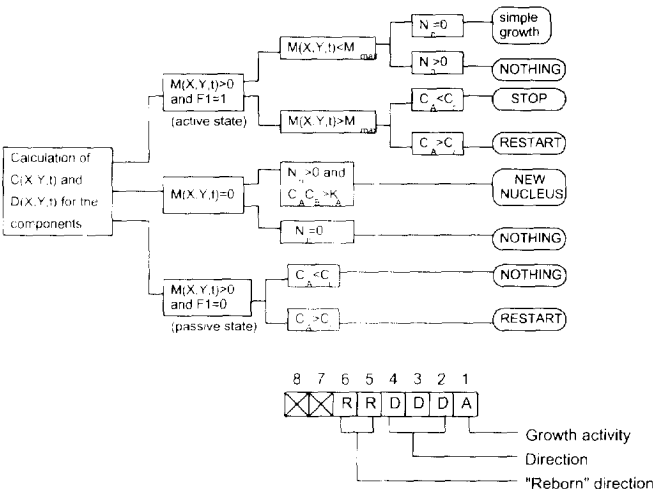

Fig. 10. An overview about the algorithm applied in simulation of tree-like Liesegang structures and the structure of the flag byte. F1 means the first bit of the flag byte. $M(X, Y, t)$ stands for the mass of the precipitate at a given point. N_n is the number of occupied neighbors. C is the concentration and D is the diffusion coefficient.

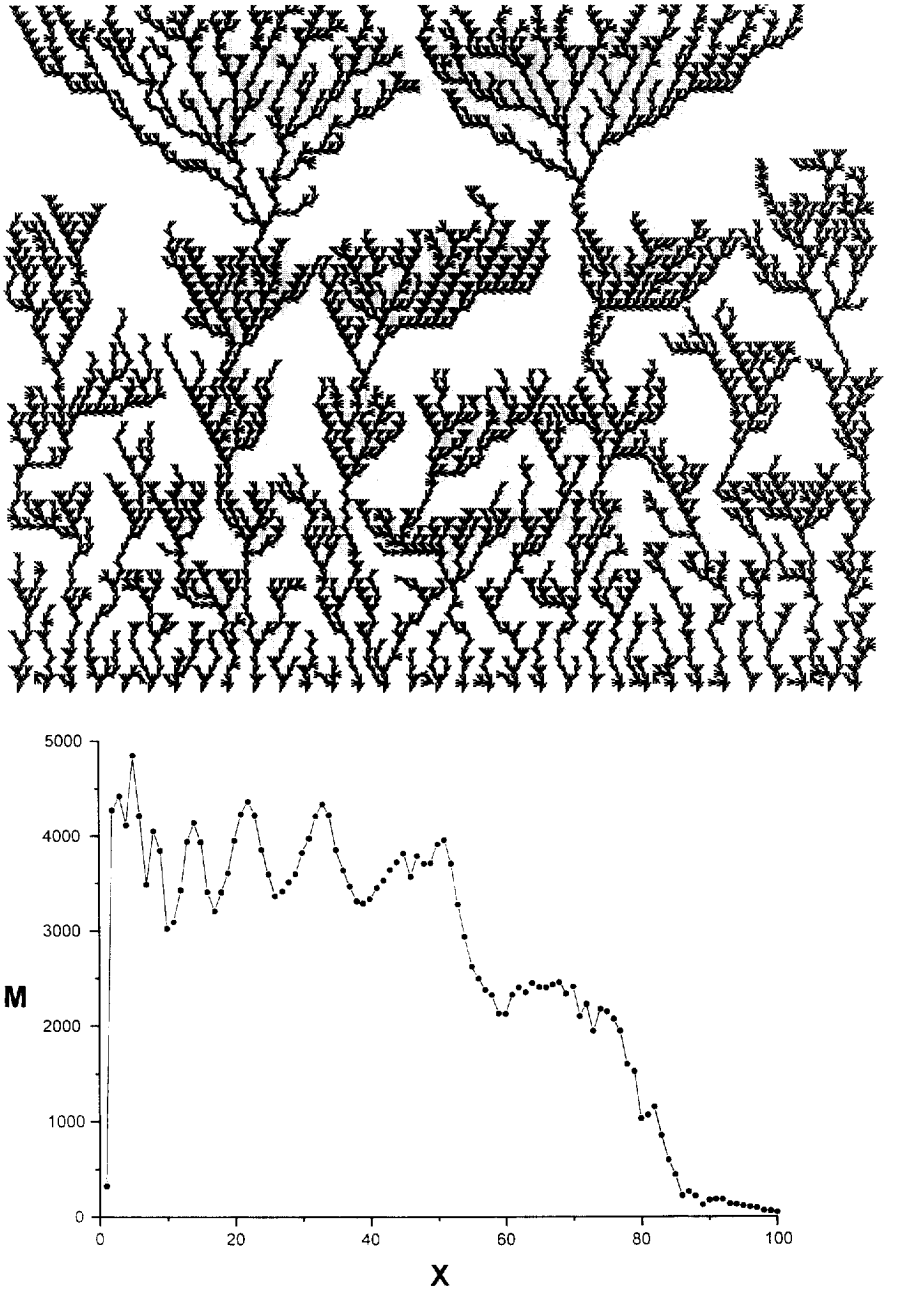

Fig. 11. A simulated tree-like precipitate pattern and its density profile. The latter was produced by adding the result of 10 runs with the same parameters.

A new crystal could be formed at a point, when the amount of the precipitate in one of the neighbouring points reached a certain value which was an input parameter. If

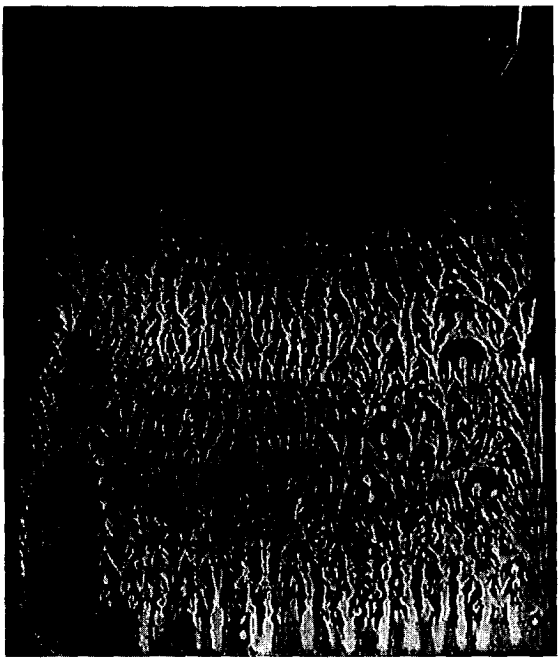

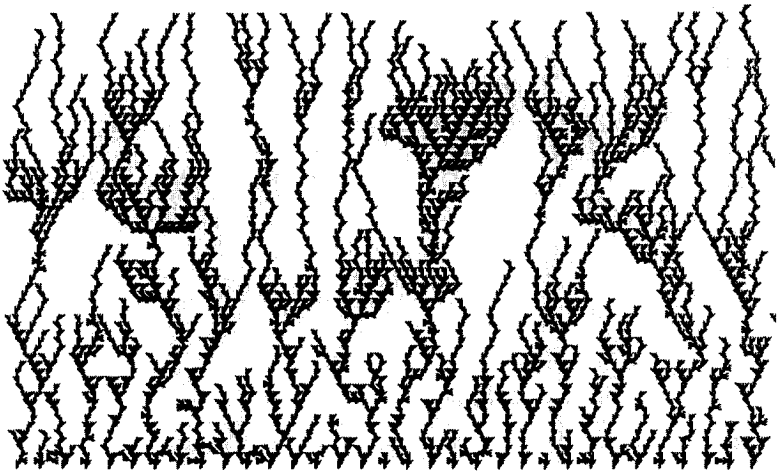

Fig. 12. An almost purely vertical structure and its simulated (counterpart).

a crystal had a new neighbour formed, its growth stopped forever (the branches can grow only at their ends).

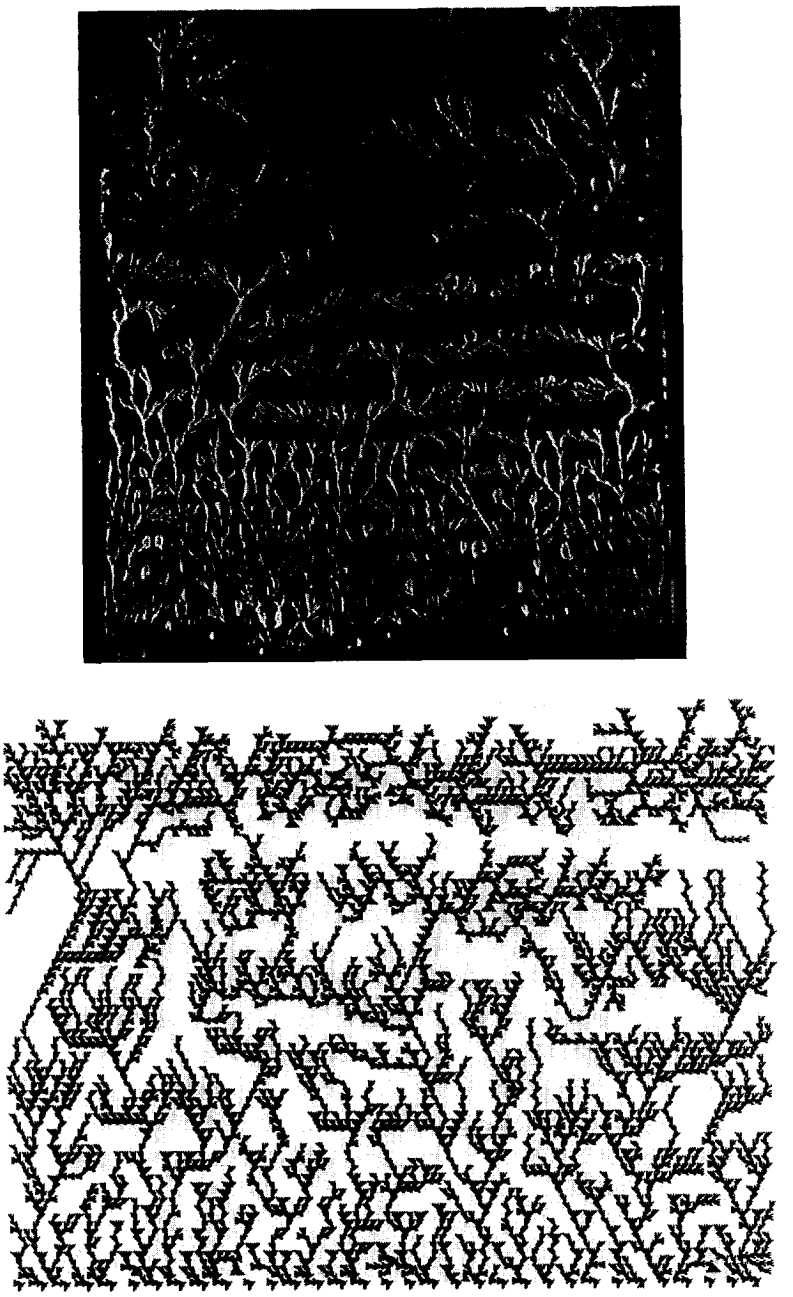

Fig. 13. A tree-like structure, which consists of purely horizontal regions, and its simulated counterpart.

The bits number 2,3 and 4 were used to mark the direction of the crystals. The lattice directions were marked from 1 to 6, so 3 bits were required to store this

information. A new nucleus could form only in those neighbouring points which were lying in the direction of the crystal. This means that a parent–child connection has been supposed between adjacent crystals.

The direction of the "child" was determined by the vectorial directions of concentration gradients. The main direction was the vectorial average of the actual gradients rounded off to a valid lattice point, however the child could vary about one direction unit, according to the decision of the random number generator. Correlation between the directions of the parent and the child was not supposed in the model. An overview of the algorithm can be seen in Fig. 10.

By means of this simulation program it was possible to reproduce the characteristic features of this anomalous structure formation. We have performed runs on 100×100 unit length sized lattices. This size was high enough to exhibit structure formation, but was too small to make an accurate density profile. However, if we added up some patterns (generally 8–10) which were simulated with the same input parameters it was possible to reconstruct the periodic density profiles. Such a simulated structue and its density waves can be seen in Fig. 11.

The whole pattern can be divided into two subsections. The arrangement of the peaks of the density profile fulfil the Jablczinsky relation individually, however there is a difference in the spacing coefficient between the two parts. This means, that a breaking point can be seen on the $\mathrm{Ln}(X_n)$ versus n plot. Our numerical model was able to reproduce even this secondary effect as can be seen in Fig. 4 on the corresponding transformed curves.

Sometimes the real pattern does not have a periodicity in its density. Branches grow almost vertically upwards and they never stop. It was possible to realize such a pattern by increasing the outer concentration. If this reaches a certain value the above-described kinetically hindered state cannot come into existence, because the concentration of the outer electrolyte at branch endings is high enough every time to prevent it. This type of a real pattern and some simulated ones can be seen in Fig. 12.

We have found some patterns which behave contrary to the one described above. In these the branches grow horizontally, which cannot be proved by the governing effect of the electrolytes. However, if we take into account only the effect of the inner one, the simulated structure will be rather horizontal just like the above-mentioned real patterns. A real pattern and a simulated one of this kind are shown in Fig. 13.

Acknowledgement

The support of Hungarian Academy of Sciences under contracts OTKA-2166 and F014023 is highly acknowledged. We also thank the J. Varga Foundation for financial support.

References

[1] A. Turing, Philos. Trans. R. Soc. B 37 (1952) 237.
[2] R.E. Liesegang, Naturw. Wochschr. 11 (1896) 353.
[3] K.H. Stern, Chem. Rev. 54 (1954) 79.
[4] H.K. Henisch, J.M. Garcia-Ruiz, J. Crystal Growth 75 (1986) 195.
[5] H.K. Henisch, J.M. Garcia-Ruiz, J. Crystal Growth 75 (1986) 203.
[6] H.K. Henisch, J. Crystal Growth, 76 (1986) 279.
[7] H.K. Henisch, Periodic Precipitation (Pergamon, New York, 1991).
[8] H.K. Henisch, Crystals in Gels and Liesegang Rings, (Cambridge Univ. Press, Cambridge, 1988).
[9] É. Kárpáti-Smidróczki, A. Büki and M. Zrínyi, J. Coll. Polym. Sci., in press.
[10] I. Dash, S. Chand and A. Pushkarna, J. Phys. Chem 93 (1989) 7435.
[11] R.P. Rastogi et al., J. Chem. Edu. 69 (1992) A 47.
[12] J.S. Kirkaldy, Rep. Prog. Phys. 55 (1992) 723.
[13] C. Wagner, J. Colloid. Sci. 5 (1950) 85.
[14] S. Kai, S.C. Müller and J. Ross, J. Chem. Phys. 73(3) (1982) 1392.
[15] J. Crank, The Mathematics of Diffusion, (Clarendon, Oxford, 1985).
[16] B. Chopard and M. Dorz, J. Stat. Phys. 64 (1991) 859.
[17] A. Büki , É. Kárpáti-Smidróczki and M. Zrínyi, submitted to J. Phys. Chem.
[18] A.L. Smith, Particle Growth in Suspensions, (Academic Press, London, 1973).
[19] M. Abdulkhadar and M.A. Ittyachan, Cryst. Res. Technol. 17 (1982) 33.